HHS Public Access

Author manuscript

Cancer Res. Author manuscript; available in PMC 2018 March 15.

Published in final edited form as:

Cancer Res. 2017 March 15; 77(6): 1331–1344. doi:10.1158/0008-5472.CAN-16-0497.

Bone metastasis of prostate cancer can be therapeutically targeted at the TBX2-WNT signaling axis

Srinivas Nandana[1,*], **Manisha Tripathi**[1,*], **Peng Duan**[1], **Chia-Yi Chu**[1], **Rajeev Mishra**[1], **Chunyan Liu**[1], **Renjie Jin**[2], **Hironobu Yamashita**[3], **Majd Zayzafoon**[4], **Neil A. Bhowmick**[1], **Haiyen E. Zhau**[1], **Robert J. Matusik**[2], and **Leland W.K. Chung**[1]

[1]Uro-Oncology Research Program, Department of Medicine, Cedars-Sinai Medical Center, Los Angeles, CA

[2]Department of Urologic Surgery, Vanderbilt University Medical Center, Nashville, TN

[3]Department of Pathology, Penn State College of Medicine, PA

[4]Department of Pathology, University of Alabama at Birmingham, AL

Abstract

Identification of factors that mediate visceral and bone metastatic spread and subsequent bone remodeling events is highly relevant to successful therapeutic intervention in advanced human prostate cancer (PCa). TBX2, a T-box family transcription factor that negatively regulates cell cycle inhibitor p21, plays critical roles during embryonic development, and recent studies have highlighted its role in cancer. Here we report that TBX2 is overexpressed in human PCa specimens and bone metastases from xenograft mouse models of human PCa. Blocking endogenous TBX2 expression in PC3 and ARCaPM PCa cell models using a dominant negative construct resulted in decreased tumor cell proliferation, colony formation, and invasion in vitro. Blocking endogenous TBX2 in human PCa mouse xenografts decreased invasion and abrogation of bone and soft tissue metastasis. Furthermore, blocking endogenous TBX2 in PCa cells dramatically reduced bone colonizing capability through reduced tumor cell growth and bone remodeling in an intra-tibial mouse model. TBX2 acted in trans by promoting transcription of the canonical WNT (WNT3A) promoter. Genetically rescuing WNT3A levels in PCa cells with endogenously blocked TBX2 partially restored the TBX2-induced PCa metastatic capability in mice. Conversely, WNT3A neutralizing antibodies or WNT antagonist SFRP-2 blocked TBX2 induced invasion. Our findings highlight TBX2 as a novel therapeutic target upstream of WNT3A, where WNT3A antagonists could be novel agents for the treatment of metastasis and for skeletal complications in PCa patients.

Keywords

prostate cancer; bone metastasis; TBX2; WNT; xenograft mouse models

Corresponding Authors: Leland W.K. Chung and Srinivas Nandana, Uro-Oncology Research Program, Department of Medicine, Samuel Oschin Comprehensive Cancer Institute, Cedars-Sinai Medical Center, 8750 Beverly Blvd, Atrium 103, Los Angeles, CA, 90048. Phone: 310-423-7622; Fax: 310-423-8543; Leland.Chung@cshs.org; Srinivas.Nandana@cshs.org.

*These authors contributed equally

Conflict of Interest: Authors have no conflict of interest to disclose.

Introduction

Prostate cancer (PCa) is the second leading cause of cancer death in men in the United States. Most patients who suffer from PCa do not die from the tumor at the primary site but rather due to complications arising from the spread of the tumor to bone and other visceral organs. Evidence indicates that only 25% of patients with metastatic and invasive PCa live 5 years subsequent to the initial diagnosis of metastasis. The spread of PCa cells to the bone and visceral organs establishes a reciprocal paracrine loop with the host organ microenvironment in a vicious cycle altering host organ homeostasis, and in the case of bone metastasis manifests as rapid cycles of new bone formation and bone destruction. Therefore, early detection and treatment before the tumors colonize the bone and visceral organs are critical for reducing the mortality and morbidity of PCa patients.

The TBX genes belong to the T-box family of transcription factors reported to play critical roles during embryonic development (1–3). Several reports have implicated TBX2 in the cell cycle and cancer; TBX2 has been shown to transcriptionally repress p14 arf/p19 arf (4,5) and p21 expression (6) and to be associated with retinoblastoma (7). In PCa, the 17q23 amplicon harboring TBX2 has been reported to be amplified in 46% of late stage hormone refractory adenocarcinomas and 31% of metastases (8).

The Wnt signaling pathway mediates a myriad of biological processes including cell proliferation and survival. Canonical Wnt signaling results in the stabilization and translocation of β-catenin to the nucleus and concomitant activation of downstream targets associated with an invasive phenotype. Several reports have documented the crucial roles played by canonical Wnt signaling in PCa tumorigenesis and metastasis.

In this report, we analyzed the specific role played by TBX2 in human PCa. By a combination of *in vitro* assays and *in vivo* xenograft experimental approaches, we focused our investigation on the biology of TBX2 in PCa progression, especially local invasion to lymph nodes and metastasis to bone, and the subsequent bone remodeling events that follow colonization and growth of PCa cells in the bone microenvironment. We found that blocking endogenous TBX2 reduces PCa cell proliferation and invasion *in vitro*, abrogates PCa metastasis to the bone, and reduces the ability of PCa cells to grow in the bone microenvironment *in vivo*. Further, we found that WNT3A signaling is an essential mediator for the effects of TBX2 in PCa metastasis, raising the possibility of targeting WNT3A by employing WNT3A neutralizing antibodies or WNT antagonist secreted frizzled receptor-2 (SFRP-2) for the management of men with locally invasive and metastatic PCa.

Materials and Methods

Tissue specimens

Thirty-five formalin-fixed, paraffin embedded (FFPE) tissues from patients with prostatic disease including nine with BPH, nine with Grade 3, ten with Grade 4 – including seven with Gleason Score 8, and seven with bone metastasis were used to determine the protein

expression of TBX2 by immunohistochemistry (IHC). Usage of clinical specimens was approved by the Institutional Research Board (IRB Protocol 00021228).

Cells and reagents

Human PCa PC3 and RWPE1 cell lines were obtained from American Type Culture Collection. Human PCa LNCaP, C4-2, C4-2B (9), $ARCaP_E$ and $ARCaP_M$ cells (10,11) were established in our laboratory between 1994 and 1996. These cell lines have been authenticated and can be obtained through characterized cell core at the University of Texas MD Anderson Cancer Center or through Novicure Biotechnology, Birmingham, AL. Luciferase tagged parental PC3 and $ARCaP_M$ cells that were stably transduced with either the control Neo or p-BABE-puro-TBX2 DN retroviral vectors were used for this study. These cells were maintained in T-medium (Invitrogen) supplemented with 5% FBS. LNCaP cells were maintained in RPMI medium supplemented with 10% FBS and were stably transduced with either the control Neo or LZRS-TBX2-ires GFP vectors. p-BABE-puro-TBX2 DN construct was provided by Colin Goding (Nuffield Department of Medicine, University of Oxford, UK), and TBX2 over-expression construct (LZRS-TBX2-iresGFP) was provided by Maarten van Lohuizen (NKI, Amsterdam). Active WNT3A vector (43810) containing Neomycin resistant gene was acquired through a Material Transfer Agreement from Addgene.

Animal Studies

All animal procedures were performed according to an approved protocol from the Institutional Animal Care and Use Committee. Male 4–6 week-old athymic nude mice, SCID-beige purchased from Charles River were housed at Cedars-Sinai Medical Center (CSMC), and fed a normal chow diet. Cells were inoculated intra-cardially or intra-tibially, or grafted beneath the kidney capsule (subrenal capsular model) or orthotopically. For metastatic studies, 1×10^6 $ARCaP_M$ cells or 2×10^5 PC3 cells tagged with a Firefly luciferase reporter construct (Promega) were injected into the left cardiac ventricle of anesthetized mice as described previously (11). Anesthetized mice were injected intra-peritoneally with 30 mg of D-Luciferin per mouse (Gold Biotech) and development of metastases was monitored by BLI on a weekly basis. Bioluminescence images were acquired using Xenogen IVIS Spectrum Imaging System (PerkinElmer) and analysis was performed with Living Image software (PerkinElmer) by the measurement of photon flux in whole mice bodies. For intra-tibial studies, 1×10^5 PC3 cells were injected in the tibia of mice and the tibia were harvested after 5 weeks. For orthotopic grafts, 1×10^6 PC3 cells were engrafted in the anterior lobe of the mouse prostates and harvested after 10 weeks of implantation. For the subrenal capsule xenograft model, 3×10^5 cells were implanted beneath the kidney capsule of mice and harvested after 8 weeks.

Microcomputed tomography (μCT) analysis

In order to determine the 3-dimensional architecture of the bone following tumor cell inoculation, mice were euthanized and the tibia were harvested and fixed overnight in 10% neutral buffered-formalin for 24 hours, followed by 70% ethanol. Bone samples were scanned using a μCT system (Scanco μCT 40; Bassersdorf, Switzerland). The scan was composed of 129 slices, with a threshold value of 263. A 3-dimensional reconstruction of

the image was performed with the region of interest consisting of trabecular bone area. Regions of interest were drawn on each of the 100 slices in such a way that only the trabecular bone and the marrow were included.

Immunohistochemistry

Immunohistochemical (IHC) analysis of tumor xenograft samples was followed a previously published protocol (12) using primary antibodies against TBX2, WNT3A, MMP9, and FOXA1. Briefly, FFPE sections (4μm) were deparaffinized, rehydrated, and subjection to antigen retrieval. Following incubation with Dual Endogenous Enzyme Block solution (Dako) for 10 minutes, the section was treated with primary antibody of varying dilutions using Antibody Diluent solution (Dako) at 4° C overnight. The section was then washed 3 times with PBST (PBS containing 0.2% Tween-20) for 5 minutes per wash. The section was then treated with EnVision + Dual Link System-HRP (Dako) for 30 min to detect specific staining. The sections were then washed 3 times for 5 minutes each, and developed with 3′3-diaminobenzidine (Dako). Image acquisition was performed using a Nikon camera and software. Magnification: x500. IHC staining intensity was scored using the combined intensity and percentage of positive-scoring cells as previously reported (13). Strong intensity was scored as 3, intermediate as 2, weak as 1, and negative as 0 Each intensity score was then summed with the percentage of cells that were stained, with >50% of the cells as 2, <50% of the cells as 1, and none as 0.

In vitro cell proliferation, colony formation and invasion assays

For cell proliferation assays, cells were seeded on 24-well plates. Cell numbers from triplicate wells were counted. For colony formation assays, 200 viable cells were seeded in 6 well plates and cultured for 10–14 days. The cell colonies were stained with crystal violet and then counted. To determine the invasive ability of PCa cells, the upper sides of the transwell polycarbonate membrane filters, with 8 mm pore size (Corning Inc, Corning, New York USA), were coated with diluted Matrigel (BD biosciences). 50,000 cells were seeded in the upper chamber with serum free media, and the bottom chamber of the apparatus contained media with 10% FBS. Cells were incubated for 48 hrs at 37°C. Following incubation, the cells that had invaded and attached to the lower surface of the membrane were fixed with 100% methanol and stained with 0.5% crystal violet. All experiments were repeated 3 times with cells grown at 37°C with 5% CO_2. Cell numbers were counted and quantified in 5 randomly chosen macroscopic fields per membrane using an inverted microscope. WNT3A (cat no MAB1324) and IL-6 (cat no MAB-206) neutralizing antibodies were obtained from R&D Systems.

Biochemical analyses

Total RNA from cells was isolated using an RNeasy Mini kit (Qiagen) and reverse transcribed to cDNA using the SuperScript III First-Strand Synthesis System (Invitrogen). Details of primers and methods used for qPCR are provided in Supplementary Materials and Methods. For immunoblots, proteins (30 μg) were resolved on a 4–12% Bis-Tris gradient SDS-PAGE under reducing conditions and transferred onto nitrocellulose membrane. The primary antibodies were TBX2, p21, WNT3A, and HA. Chromatin Immunoprecipitation (ChIP) assay in PC3 cells to determine the binding of TBX2 on WNT3A promoter was

performed using ChIP assay kit (Upstate Biotechnology) following the manufacturer's protocol. ChIP DNA was analyzed by PCR analysis using primers encompassing the regions of interest on WNT3A promoter. ChIP in LNCaP cells was performed using the Zymo-Spin kit (Zymo Research) following the manufacturer's protocol. Details of primers used for ChIP are provided in Supplementary Materials and Methods.

Statistics

GraphPad Prism 6 was used for graphs and statistics. Data was expressed as a mean ± SE. All data was analyzed using the Student *t* test for comparison of two groups or one-way ANOVA for three groups or more. Differences were considered statistically significant when the *P* value was <0.05.

Results

TBX2 is overexpressed in human PCa cell lines, tumor xenografts and clinical specimens, and its expression correlates with the potential to metastasize to bone and soft tissues

We evaluated TBX2 expression in human PCa cell lines, PCa tumor xenografts and PCa clinical specimens with the goals of assessing the relationship between TBX2 expression and the ability of PCa cells to home to bone and soft tissues. In addition, we examined the potential correlation of TBX2 expression in pathologic PCa specimens collected from patients with various stages of the disease. Three bone metastatic human PCa cell lines and tumor xenografts with lineage relationships, LNCaP-C4-2-C4-2B (14), LNCaP ^{Neo}-LNCaP ^{RANKL} (15) and ARCaP$_E$-ARCaP$_M$ (16), were chosen for this study. We found that TBX2 expression in these PCa cell lines (Fig 1, Panels D and E) and xenografts (Fig 1, Panel A) correlated with their bone and soft tissue metastatic potential. TBX2 expression and its association with cell nucleus in C4-2B, LNCaP ^{RANKL} and ARCaP$_M$ tumors was higher than those of the respective lineage-related tumors derived from the parental cell lines LNCaP, LNCaP ^{Neo} and ARCaP$_E$ cells (Fig 1, Panels A, D, and E). We observed a correlation between TBX2 and WNT3A protein expression in three bone metastatic human PCa cell lines with lineage relationships - LNCaP-C4-2B, ARCaP$_E$-ARCaP$_M$ and PC3-PC3M (Supplementary Fig 1). We found that TBX2 expression was higher in human PCa clinical specimens and increased with disease progression (Fig 1, Panels B and C). In addition, we evaluated TBX2 expression in a number of human PCa microarray data sets using Oncomine 4.4. Using Cancer Outlier Profile Analysis (COPA), a methodology that has been validated for the identification of candidate oncogenes such as ERG (17), we found that TBX2 is significantly over-expressed in a subset of tumor samples in 11 out of 23 available data sets (gene rank, top 20%; fold change > 2; $P < 1\times 10^{-4}$) (Supplementary Table 1). Our results are consistent with a previous report where TBX2 was found to be highly overexpressed in osteoblastic bone metastases in patients with castration-resistant prostate cancer (CRPC) (18). Taken together, these results show that TBX2 has a preferential expression in PCa bone metastases and that TBX2 expression increases with human PCa progression.

Identification of WNT3A and MMP9 as downstream effectors of the TBX2 signaling axis

To understand the biological role of TBX2 in PCa growth and metastasis, we took a genetic approach by blocking endogenous TBX2 expression in PCa cells using a dominant negative construct (TBX2 DN) that comprises of a deletion mutant that includes amino acids 1–301. This TBX2 DN construct contains the T-box DNA binding domain, but lacks the carboxy-terminal residues necessary for transcriptional repression. A previous study assessing the functional role of TBX2 in melanoma successfully used the TBX2 DN construct and reported that TBX2 DN works in congruence with TBX2 siRNA and up-regulates p21, a known TBX2 target. (6). Further, deletion mutants designed in this manner have been previously demonstrated to act as dominant negative for several other genes of the T-box family in a variety of tissues and organisms (19,20). TBX2 DN expression in PCa cells decreased the ability of PC3 and $ARCaP_M$ cells to proliferate and to form soft agar colonies (Fig 2, Panels A and B). Cells transduced with TBX2 DN construct had greater expression of p21 (Fig 2, Panel D), in agreement with the function of this construct in human melanoma cells (6). We screened expression of both canonical and non-canonical WNTs in PCa cells expressing TBX2 DN. Results showed that the TBX2 DN construct decreased a canonical WNT, WNT3A, in both PC3 and $ARCaP_M$ cells (Figure 2, Panel C). Further, the expression of MMP9, a known target downstream from WNT3A signaling, was decreased in PCa cells expressing TBX2 DN construct (Figure 2, Panel C). In addition, utilizing the converse approach, we found that LNCaP human PCa cells transduced with TBX2 over-expression construct ($LNCaP^{TBX2}$) displayed increased WNT3A and MMP9 levels compared with control $LNCaP^{Neo}$ cells (Supplementary Fig 2, Panel A). These results taken together suggested that the TBX2 downstream signaling axis involves WNT3A, MMP9, and p21 gene expression in PCa cells.

TBX2 contributes to local tumor invasion and distant metastasis

The functional effects of the TBX2 DN construct on the invasion and metastasis of PC3 and $ARCaP_M$ cells *in vitro* and *in vivo* were investigated. TBX2 DN stable infection dramatically reduced the invasive behavior of PC3 and $ARCaP_M$ cells. Modified Boyden chamber assays showed dramatically reduced invasive capabilities of these cells when compared with respective cells stably transduced with the control vector (Fig 3, Panel A; Supplementary Fig 3). These results were corroborated by the *in vivo* behaviors of sub-renal implanted PC3 cells transduced with TBX2 DN construct ($PC3^{TBX2\ DN}$). In order to differentiate the tumor xenograft from the kidney tissue we stained the tumor xenograft sections with FOXA1 since PC3 tumors stain positive for FOXA1 while the there is no detectable staining in the kidney tissue. We observed that the TBX2 DN construct dramatically reduced the invasive front of the tumor as seen in the boundaries clearly demarcated in tumor and kidney (Fig 3, Panel B, highlighted by arrows and a dotted line). Interestingly, while tumor invasiveness was greatly decreased, the TBX2 DN construct did not affect the growth and the size of PC3 tumors in mice (data not shown). As expected, $PC3^{TBX2\ DN}$ tumors lost the expression of WNT3A and MMP9, two of the downstream target genes of TBX2. While strong WNT3A and MMP9 staining was evident in control $PC3^{Neo}$ tumors, $PC3^{TBX2\ DN}$ tumors demonstrated a significant loss of WNT3A and MMP9 (Fig 3, Panel C). To further examine the functional significance of TBX2 in PCa invasion in the prostate microenvironment, we compared local invasion and lymph node metastases in an

orthotopic xenograft model where mouse prostate glands were inoculated with either TBX2 DN or control transduced PC3 cells. Orthotopically implanted PC3 cells have been observed to invade locally and metastasize readily to adjacent lymph nodes (21–23). Consistent with data from the kidney capsule tumor xenograft study, orthotopically implanted PC3 $^{TBX2\ DN}$ cells exhibited drastically reduced local invasion with no evidence of lymph node metastases (Fig 3, Panel D highlighted by arrows), while control PC3 ^{Neo} tumors showed local invasion and regional lymph node metastasis. Taken together, these results further support the finding that TBX2 plays a critical role in PCa local invasion and distant metastases to lymph nodes in mouse models.

Dominant negative TBX2 expression in PCa cells abrogates cancer bone metastasis

Since bone is the predominant metastatic site in human PCa, we next investigated if TBX2 expression had a role in the manifestation of PCa bone metastasis. $ARCaP_M$ and PC3 cells known for their ability to metastasize spontaneously to mouse skeleton, were used as models to evaluate the functional role of TBX2 in PCa cells. Intra-cardiac inoculation of control vector transduced $ARCaP_M$ cells ($ARCaP_M^{Neo}$) resulted in a bone metastatic frequency of 80% during an 8-week observation period (Fig 4, Panel A), while control PC3 ^{Neo} cells resulted in a bone metastasis frequency of 60% during a 6-week observation period (Fig 4, Panel B). In sharp contrast, $ARCaP_M^{TBX2\ DN}$ and PC3 $^{TBX2\ DN}$ cells failed to exhibit any signs of bone and soft tissue metastases, even when the observation period was extended to 12 weeks. We confirmed bone and soft tissue metastases in mice using bioluminescence imaging, and additionally confirmed metastasis by X-ray and micro-CT (data not shown) and H/E analysis of the harvested tissue specimens (Fig 4, Panel D). These results taken together strongly support the role played by TBX2 in mediating PCa bone and soft tissue metastasis in mouse models.

Dominant negative TBX2 alters PCa bone remodeling

To determine if TBX2 could exert direct bone remodeling effects on mouse skeleton, we inoculated both PC3 $^{TBX2\ DN}$ and control PC3 ^{Neo} cells in mouse skeleton and compared the histopathology and IHC characteristics of the tumor xenografts grown in mouse skeleton. As expected, intra-tibial injection of PC3 ^{Neo} cells gave rise to extensive osteolysis, with extensive loss of trabecular bone at the site of tumor cell inoculation (Fig 5). In contrast, PC3 $^{TBX2\ DN}$ cells gave rise to mild osteolysis as seen by X-ray and confirmed by micro-CT analysis (Fig 5). Further, significantly smaller tumors were observed in mouse skeletons inoculated intra-osseously with PC3 $^{TBX2\ DN}$ cells when compared with PC3 ^{Neo} tumors (Fig 5). We performed a similar experiment with $ARCaP_M$ cells, which form a mixture of osteolytic and osteoblastic lesions. Consistent with the PC3 tumors in mouse skeleton, when compared with $ARCaP_M^{Neo}$ cells, $ARCaP_M^{TBX2\ DN}$ cells also formed smaller tumors with significantly reduced potential to remodel the bone microenvironment, manifested by reduced osteolysis and osteoblastic lesions (Supplementary Fig 4).

WNT3A, a downstream target gene of TBX2, mediates PCa bone metastasis

Since we observed downregulated WNT3A in PCa cells transduced with TBX2 DN, we determined the possible functional role of WNT3A in mediating PCa metastasis. We therefore generated stable WNT3A-expressing PC3 cells that had previously been

transduced with TBX2 DN (PC3 $^{TBX2\ DN\ +\ WNT3A}$ cells). To examine the phenotypic behavior of these cells with respect to the behavior associated with WNT3A or its downstream effectors, we treated all three types of cells - PC3^{Neo}, PC3 $^{TBX2\ DN}$ and PC3 $^{TBX2\ DN\ +\ WNT3A}$ with *1)* WNT3A neutralizing antibody, or *2)* SFRP-2 or, *3)* IL6 neutralizing antibody, and examined the invasive behavior of the cells. *In vitro* Boyden chamber assays showed that *1)* PC3 $^{TBX2\ DN\ +\ WNT3A}$ cells displayed significantly enhanced invasion compared with PC3 $^{TBX2\ DN}$ cells and, *2)* While treatments with WNT3A neutralizing antibody or SFRP-2 or IL6 neutralizing antibody drastically reduced the invasive behavior of PC3 ^{Neo} and PC3 $^{TBX2\ DN\ +\ WNT3A}$ cells, the invasive behavior of PC3 $^{TBX2\ DN}$ cells did not change significantly (Fig 6 Panel A, Supplementary Fig 5). Quantitative real-time RT-PCR confirmed that WNT3A expression as well as MMP9, MMP2 and IL6, genes known to be downstream of WNT3A were rescued in PC3 $^{TBX2\ DN\ +\ WNT3A}$ compared with PC3 $^{TBX2\ DN}$ cells (Fig 6, Panel B). Conversely, Boyden chamber assays showed that while LNCaP ^{TBX2} cells displayed a significant increase in invasive behavior compared with control LNCaP ^{Neo} cells, addition of WNT3A neutralizing antibody decreased the invasive ability of LNCaP ^{TBX2} cells (Supplementary Fig 2, Panel B).

To further tease out the *in vivo* biological consequences of WNT3A rescue in the context of blocking endogenous TBX2, we injected all three types of cells PC3 ^{Neo}, PC3 $^{TBX2\ DN}$ and PC3 $^{TBX2\ DN\ +\ WNT3A}$ by intra-cardiac inoculation in immune-deficient mice. Bioluminescence imaging revealed that mice injected with PC3 $^{TBX2\ DN+\ WNT3A}$ cells had partially restored bone and soft tissue metastatic potential (Fig 6, Panel C), when compared with mice injected with PC3 $^{TBX2\ DN}$ cells which, as shown previously, did not show any evidence of metastasis.

We next investigated the molecular mechanisms by which TBX2 regulated WNT3A. We used chromatin immunoprecipitation (ChIP) assay to determine if there is a differential recruitment of TBX2 to WNT3A promoter in PC3 ^{Neo} and PC3 $^{TBX2\ DN}$ cells. The results showed that binding of TBX2 on WNT3A promoter was significantly diminished in PC3 $^{TBX2\ DN}$ cells when compared to control PC3 ^{Neo} cells (Fig 6, Panel D). These results collectively suggest that the diminished binding of TBX2 on WNT3A promoter that occurs in PC3 $^{TBX2\ DN}$ cells leads to decreased expression of WNT3A. To further validate this finding, we examined whether TBX2 activation led to the recruitment of RNA polymerase II (Pol II) to the WNT3A promoter. We observed that recruitment of Pol II to the WNT3A promoter was decreased in PC3 $^{TBX2\ DN}$ cells compared with control PC3 ^{Neo} cells (Fig 6, Panel D; Supplementary Fig 6, Panel A), implying that blocking TBX2 leads to a significant decrease in WNT3A promoter activity. Utilizing an alternative approach, we observed enhanced TBX2 binding on WNT3A promoter in LNCaP ^{TBX2} cells compared with LNCaP ^{Neo} cells (Supplementary Fig 6, Panels A and B). Overall, the ChIP data reveal a mechanism of WNT3A regulation by TBX2, and the experiments with rescue of WNT3A expression in the context of blocking endogenous TBX2 demonstrate that *1)* the expression and phenotypic properties - *in vitro* invasion - associated with WNT3A and its downstream effectors like MMP9, MMP2 and IL6 are restored in PC3 $^{TBX2\ DN\ +\ WNT3A}$ cells compared with PC3 $^{TBX2\ DN}$ cells and, *2) in vivo* metastatic behavior is partially rescued in PC3 $^{TBX2\ DN\ +\ WNT3A}$ cells when compared with PC3 $^{TBX2\ DN}$ cells.

In summary, our data suggests that TBX2 expression is increased in PCa bone metastatic tumor xenograft samples and in clinical high Gleason grade PCa samples. Our data further shows that increased TBX2 in PCa activates an invasive and metastatic behavior in PCa cells that is mediated by WNT3A and its downstream effectors, MMP9, MMP2 and IL-6 (Fig 7).

Discussion

The widespread clinical manifestation of bone metastases in PCa patients is the leading cause of mortality as well as loss in quality of life. However, the genetic mechanisms that mediate the process of metastatic bone colonization and subsequent growth in the bone microenvironment remain poorly defined. In this study, we show the first evidence of a coordinated regulation of PCa bone metastasis mediated by TBX2 through its downstream effectors WNT3A, MMPs and IL-6.

Of relevance to our study, a previous report identified TBX2 as well as TCF4, an effector of the canonical WNT signaling pathway, to be highly overexpressed in osteoblastic bone metastases in patients with CRPC (18). In agreement with that study, we confirmed TBX2 overexpression in: *1)* the more aggressive androgen independent and metastatic variants of PCa cell lines, *2)* bone metastatic specimens obtained from mice inoculated with aggressive human PCa cells, and *3)* localized and metastatic human PCa tissues.

Work done in the past decade has shown that bone metastasis in PCa is a complex process that broadly involves 3 steps: *1)* malignant progression of the primary tumor and invasion through the surrounding extra-cellular matrix to reach the blood stream, *2)* PCa cells traveling in the blood stream and homing to the bone through extravasation, and *3)* interaction of the colonized PCa cells with the bone microenvironment to produce mixed lesions - bone resorption or osteolysis along with concomitant new bone formation or osteopetrosis. Utilizing a series of xenograft mouse models, our results consistently show that TBX2 plays a seminal role in mediating all three steps in the metastatic cascade. Further, our results from the orthotopic xenograft technique (that physiologically mimics the primary organ microenvironment) showing that blocking TBX2 expression abrogates PCa lymph node metastasis are consistent with our data from the experimental metastasis model.

In addition to understanding PCa cell homing to the bone, it is paramount to decipher the molecular mechanisms that determine PCa cell interactions with the bone microenvironment. It is well known that reciprocal interactions between the bone microenvironment and the colonizing tumor cells brings about bone remodeling, a process that leads to the painful complications associated with bone metastasis in PCa patients. Our data shows that blocking endogenous TBX2 greatly reduces growth in the bone microenvironment as demonstrated by the intra-tibial xenograft model utilizing both PC3 and $ARCaP_M$ cells. Although PCa bone metastases are predominantly osteoblastic, several studies have strongly suggested that the successful colonization of the bone by PCa cells encompasses both osteolytic and osteoblastic events, and that the initial colonization step leads to a lytic lesion (24–28). These observations are in accord with and appropriately reflected by the models we used in our study; while the bone lesions formed by PC3 cells

are highly osteolytic, $ARCaP_M$ cells on the other hand form a mixture of lytic and blastic lesions in the bone.

Several studies have demonstrated that WNT signaling is positively correlated with PCa progression and a few have shown its direct role in inducing bone metastasis (29–35). Most notably, a recent large multi-institutional whole exome and transcriptome sequencing study of bone and soft tissue biopsies from 150 metastatic CRPC patients found alterations in the WNT signaling pathway in 18% of the cases (36). WNT3A levels are upregulated in human PCa cell lines and WNT3A has been reported to induce PCa bone metastasis through the regulation of BMPs (37,38). WNT3A neutralizing antibodies injected intraperitoneally have been shown to decrease proliferation and induce apoptosis in a PCa mouse model (39), and the WNT antagonist SFRP-2 has been shown to inhibit WNT3A *in vivo* (40). Further, WNT3A is reported to induce IL-6 expression (41). High circulating levels of IL-6 have been associated with adverse clinical outcomes in patients with metastatic CRPC (42) and targeting IL-6 signaling has been shown to inhibit PCa growth in the bone (43). In addition, WNT3A is reported to regulate MMPs 2 and 9 (44), the extracellular matrix components that bring about the degradation of basement membrane and are known to play seminal roles in PCa invasion and metastasis (45). Additionally, high levels of MMP2 and MMP9 in the plasma and urine of PCa patients have been shown to correlate with PCa metastasis (46,47); and IL-6 has been shown to regulate MMP9 expression (48). Taken together, these reports are in congruence with our findings that *1)* addition of WNT3A neutralizing antibodies, or the WNT antagonist SFRP-2, or IL-6 neutralizing antibodies decreased the *in vitro* invasiveness of PCa cells in the context of high TBX2 or WNT3A expression; and *2)* blocking TBX2 abrogates PCa bone metastasis in mouse xenograft models in the context of decreased expression of WNT3A, MMPs and IL-6; and that rescuing WNT3A levels in these cells partially rescues their metastatic ability with concomitant increase in the expression of MMPs and IL-6.

Our results highlight a new and specific function of TBX2 in regulating WNT3A at the transcriptional level. In congruity with our findings, a previous study identified WNT3A as a target of Brachyury (T), a transcription factor that shares the same consensus T-box binding element with TBX2 (49). Of note, TBX2 has been reported to function both as a strong repressor, and a relatively weak activator (50). In our studies since we are examining the function of TBX2 as an activator of WNT3A transcription, we think this could explain the observed weak binding of TBX2 on WNT3A promoter. However, our data demonstrates that despite the relatively weak activation, WNT3A mediates the biological function of TBX2 in the manifestation of PCa metastasis, since rescuing WNT3A levels in the context of blocking endogenous TBX2 levels in PC3 cells partially restores the metastatic ability of these cells.

It is important to underscore the reported correlation that genes and signaling pathways that play vital roles during embryonic development are often found to be dysregulated in tumor progression and metastasis. TBX2 seems to fit in the profile of these genes since previous reports have reported the role played by TBX2 in embryonic development. Interestingly, we have observed that TBX2 expression is detected very early in mouse prostate development, as early as E16 (data not shown). In addition, interestingly, our studies point to the fact that

TBX2 primarily mediates invasion and metastasis, rather than tumor growth *in vivo*. This is because despite differences in proliferation of prostate cancer cells *in vitro* upon blocking endogenous TBX2, our observations both in the kidney capsule and orthotopic xenograft mouse models demonstrate that genetically modulating TBX2 has no statistical differences in the *in vivo* tumor size. We speculate that this anomaly could be due to the presence of additional factors in the ecosystem of *in vivo* tumors such as reciprocal interactions between the tumor cells and the cells of the tumor microenvironment.

Designing novel therapeutic approaches against PCa bone metastasis based on the inhibition of WNT signaling offers potent advantages given WNT's widely reported role in PCa bone metastasis and bone remodeling events. Our model suggests that increased expression of TBX2 promotes bone metastasis and growth in the bone microenvironment through the regulation of downstream WNT3A. We posit that this newly uncovered TBX2-WNT3A signaling pathway represents a novel and exciting opportunity for the development of novel therapies targeting PCa bone metastasis.

Supplementary Material

Refer to Web version on PubMed Central for supplementary material.

Acknowledgments

Financial Support: This work was supported by NIH/NCI grants 5P01CA098912 and R01CA122602, the Board of Governors Cancer Research Chair, and the Steven Spielberg Fund in Prostate Cancer Research (to L.W.K. Chung); NCI grant R01CA076142 (to R.J. Matusik); Department of Defense Prostate Cancer Research Program grants X81XWH-07-1-0155 and X81XWH-12-1-0042 (to S. Nandana).

We thank Dr. Colin Goding (Ludwig Cancer Research, University of Oxford, UK) and Dr. Maarten van Lohuizen (NKI, Amsterdam) for kindly gifting us with the p-BABE-puro-TBX2 DN and LZRS-TBX2-iresGFP constructs respectively; and Tom Case (Department of Urologic Surgery, Vanderbilt University Medical Center) for providing technical assistance. We thank the support from the Biobank & Translational Research Core, and the Biostatistics & Bioinformatics Core at Cedars-Sinai Medical Center. We also thank Dr. Michael Freeman (Department of Surgery, Cedars-Sinai Medical Center) for critical reading of the manuscript, and Gary Mawyer for editorial assistance.

References

1. Douglas NC, Heng K, Sauer MV, Papaioannou VE. Dynamic expression of Tbx2 subfamily genes in development of the mouse reproductive system. Developmental dynamics: an official publication of the American Association of Anatomists. 2012; 241:365–75. [PubMed: 22223620]
2. Greulich F, Rudat C, Kispert A. Mechanisms of T-box gene function in the developing heart. Cardiovascular research. 2011; 91:212–22. [PubMed: 21498422]
3. Cho GS, Choi SC, Park EC, Han JK. Role of Tbx2 in defining the territory of the pronephric nephron. Development. 2011; 138:465–74. [PubMed: 21205791]
4. Jacobs JJ, Keblusek P, Robanus-Maandag E, Kristel P, Lingbeek M, Nederlof PM, et al. Senescence bypass screen identifies TBX2, which represses Cdkn2a (p19(ARF)) and is amplified in a subset of human breast cancers. Nature genetics. 2000; 26:291–9. [PubMed: 11062467]
5. Lingbeek ME, Jacobs JJ, van Lohuizen M. The T-box repressors TBX2 and TBX3 specifically regulate the tumor suppressor gene p14ARF via a variant T-site in the initiator. The Journal of biological chemistry. 2002; 277:26120–7. [PubMed: 12000749]
6. Vance KW, Carreira S, Brosch G, Goding CR. Tbx2 is overexpressed and plays an important role in maintaining proliferation and suppression of senescence in melanomas. Cancer research. 2005; 65:2260–8. [PubMed: 15781639]

7. Vance KW, Shaw HM, Rodriguez M, Ott S, Goding CR. The retinoblastoma protein modulates Tbx2 functional specificity. Molecular biology of the cell. 2010; 21:2770–9. [PubMed: 20534814]
8. Andersen CL, Monni O, Wagner U, Kononen J, Barlund M, Bucher C, et al. High-throughput copy number analysis of 17q23 in 3520 tissue specimens by fluorescence in situ hybridization to tissue microarrays. The American journal of pathology. 2002; 161:73–9. [PubMed: 12107091]
9. Thalmann GN, Anezinis PE, Chang SM, Zhau HE, Kim EE, Hopwood VL, et al. Androgen-independent cancer progression and bone metastasis in the LNCaP model of human prostate cancer. Cancer research. 1994; 54:2577–81. [PubMed: 8168083]
10. Zhau HY, Chang SM, Chen BQ, Wang Y, Zhang H, Kao C, et al. Androgen-repressed phenotype in human prostate cancer. Proceedings of the National Academy of Sciences of the United States of America. 1996; 93:15152–7. [PubMed: 8986779]
11. Xu J, Wang R, Xie ZH, Odero-Marah V, Pathak S, Multani A, et al. Prostate cancer metastasis: role of the host microenvironment in promoting epithelial to mesenchymal transition and increased bone and adrenal gland metastasis. The Prostate. 2006; 66:1664–73. [PubMed: 16902972]
12. Zhau HE, Odero-Marah V, Lue HW, Nomura T, Wang R, Chu G, et al. Epithelial to mesenchymal transition (EMT) in human prostate cancer: lessons learned from ARCaP model. Clinical & experimental metastasis. 2008; 25:601–10. [PubMed: 18535913]
13. De Marzo AM, Knudsen B, Chan-Tack K, Epstein JI. E-cadherin expression as a marker of tumor aggressiveness in routinely processed radical prostatectomy specimens. Urology. 1999; 53:707–13. [PubMed: 10197845]
14. Wu TT, Sikes RA, Cui Q, Thalmann GN, Kao C, Murphy CF, et al. Establishing human prostate cancer cell xenografts in bone: induction of osteoblastic reaction by prostate-specific antigen-producing tumors in athymic and SCID/bg mice using LNCaP and lineage-derived metastatic sublines. International journal of cancer Journal international du cancer. 1998; 77:887–94. [PubMed: 9714059]
15. Chu GC, Zhau HE, Wang R, Rogatko A, Feng X, Zayzafoon M, et al. RANK- and c-Met-mediated signal network promotes prostate cancer metastatic colonization. Endocrine-related cancer. 2014; 21:311–26. [PubMed: 24478054]
16. Odero-Marah VA, Wang R, Chu G, Zayzafoon M, Xu J, Shi C, et al. Receptor activator of NF-kappaB Ligand (RANKL) expression is associated with epithelial to mesenchymal transition in human prostate cancer cells. Cell research. 2008; 18:858–70. [PubMed: 18645583]
17. Tomlins SA, Rhodes DR, Perner S, Dhanasekaran SM, Mehra R, Sun XW, et al. Recurrent fusion of TMPRSS2 and ETS transcription factor genes in prostate cancer. Science. 2005; 310:644–8. [PubMed: 16254181]
18. Li ZG, Mathew P, Yang J, Starbuck MW, Zurita AJ, Liu J, et al. Androgen receptor-negative human prostate cancer cells induce osteogenesis in mice through FGF9-mediated mechanisms. The Journal of clinical investigation. 2008; 118:2697–710. [PubMed: 18618013]
19. Carlson H, Ota S, Campbell CE, Hurlin PJ. A dominant repression domain in Tbx3 mediates transcriptional repression and cell immortalization: relevance to mutations in Tbx3 that cause ulnar-mammary syndrome. Human molecular genetics. 2001; 10:2403–13. [PubMed: 11689487]
20. Rallis C, Bruneau BG, Del Buono J, Seidman CE, Seidman JG, Nissim S, et al. Tbx5 is required for forelimb bud formation and continued outgrowth. Development. 2003; 130:2741–51. [PubMed: 12736217]
21. Pettaway CA, Pathak S, Greene G, Ramirez E, Wilson MR, Killion JJ, et al. Selection of highly metastatic variants of different human prostatic carcinomas using orthotopic implantation in nude mice. Clinical cancer research: an official journal of the American Association for Cancer Research. 1996; 2:1627–36. [PubMed: 9816342]
22. Kozlowski JM, Fidler IJ, Campbell D, Xu ZL, Kaighn ME, Hart IR. Metastatic behavior of human tumor cell lines grown in the nude mouse. Cancer research. 1984; 44:3522–9. [PubMed: 6744277]
23. Eastham JA, Grafton W, Martin CM, Williams BJ. Suppression of primary tumor growth and the progression to metastasis with p53 adenovirus in human prostate cancer. The Journal of urology. 2000; 164:814–9. [PubMed: 10953161]

24. Garnero P, Buchs N, Zekri J, Rizzoli R, Coleman RE, Delmas PD. Markers of bone turnover for the management of patients with bone metastases from prostate cancer. British journal of cancer. 2000; 82:858–64. [PubMed: 10732759]
25. Inoue H, Nishimura K, Oka D, Nakai Y, Shiba M, Tokizane T, et al. Prostate cancer mediates osteoclastogenesis through two different pathways. Cancer letters. 2005; 223:121–8. [PubMed: 15890244]
26. Zhang J, Dai J, Qi Y, Lin DL, Smith P, Strayhorn C, et al. Osteoprotegerin inhibits prostate cancer-induced osteoclastogenesis and prevents prostate tumor growth in the bone. The Journal of clinical investigation. 2001; 107:1235–44. [PubMed: 11375413]
27. Mori K, Le Goff B, Charrier C, Battaglia S, Heymann D, Redini F. DU145 human prostate cancer cells express functional receptor activator of NFkappaB: new insights in the prostate cancer bone metastasis process. Bone. 2007; 40:981–90. [PubMed: 17196895]
28. Yonou H, Ochiai A, Goya M, Kanomata N, Hokama S, Morozumi M, et al. Intraosseous growth of human prostate cancer in implanted adult human bone: relationship of prostate cancer cells to osteoclasts in osteoblastic metastatic lesions. The Prostate. 2004; 58:406–13. [PubMed: 14968441]
29. Zhu H, Mazor M, Kawano Y, Walker MM, Leung HY, Armstrong K, et al. Analysis of Wnt gene expression in prostate cancer: mutual inhibition by WNT11 and the androgen receptor. Cancer research. 2004; 64:7918–26. [PubMed: 15520198]
30. Robinson DR, Zylstra CR, Williams BO. Wnt signaling and prostate cancer. Current drug targets. 2008; 9:571–80. [PubMed: 18673243]
31. Thiele S, Rauner M, Goettsch C, Rachner TD, Benad P, Fuessel S, et al. Expression profile of WNT molecules in prostate cancer and its regulation by aminobisphosphonates. Journal of cellular biochemistry. 2011; 112:1593–600. [PubMed: 21344486]
32. Verras M, Sun Z. Roles and regulation of Wnt signaling and beta-catenin in prostate cancer. Cancer letters. 2006; 237:22–32. [PubMed: 16023783]
33. Bruxvoort KJ, Charbonneau HM, Giambernardi TA, Goolsby JC, Qian CN, Zylstra CR, et al. Inactivation of Apc in the mouse prostate causes prostate carcinoma. Cancer research. 2007; 67:2490–6. [PubMed: 17363566]
34. Yu X, Wang Y, DeGraff DJ, Wills ML, Matusik RJ. Wnt/beta-catenin activation promotes prostate tumor progression in a mouse model. Oncogene. 2011; 30:1868–79. [PubMed: 21151173]
35. Bisson I, Prowse DM. WNT signaling regulates self-renewal and differentiation of prostate cancer cells with stem cell characteristics. Cell research. 2009; 19:683–97. [PubMed: 19365403]
36. Robinson D, Van Allen EM, Wu YM, Schultz N, Lonigro RJ, Mosquera JM, et al. Integrative clinical genomics of advanced prostate cancer. Cell. 2015; 161:1215–28. [PubMed: 26000489]
37. Hall CL, Bafico A, Dai J, Aaronson SA, Keller ET. Prostate cancer cells promote osteoblastic bone metastases through Wnts. Cancer research. 2005; 65:7554–60. [PubMed: 16140917]
38. Dai J, Hall CL, Escara-Wilke J, Mizokami A, Keller JM, Keller ET. Prostate cancer induces bone metastasis through Wnt-induced bone morphogenetic protein-dependent and independent mechanisms. Cancer research. 2008; 68:5785–94. [PubMed: 18632632]
39. Li X, Placencio V, Iturregui JM, Uwamariya C, Sharif-Afshar AR, Koyama T, et al. Prostate tumor progression is mediated by a paracrine TGF-beta/Wnt3a signaling axis. Oncogene. 2008; 27:7118–30. [PubMed: 18724388]
40. Galli LM, Barnes T, Cheng T, Acosta L, Anglade A, Willert K, et al. Differential inhibition of Wnt-3a by Sfrp-1, Sfrp-2, and Sfrp-3. Developmental dynamics: an official publication of the American Association of Anatomists. 2006; 235:681–90. [PubMed: 16425220]
41. Aumiller V, Balsara N, Wilhelm J, Gunther A, Konigshoff M. WNT/beta-catenin signaling induces IL-1beta expression by alveolar epithelial cells in pulmonary fibrosis. American journal of respiratory cell and molecular biology. 2013; 49:96–104. [PubMed: 23526221]
42. George DJ, Halabi S, Shepard TF, Sanford B, Vogelzang NJ, Small EJ, et al. The prognostic significance of plasma interleukin-6 levels in patients with metastatic hormone-refractory prostate cancer: results from cancer and leukemia group B 9480. Clinical cancer research: an official journal of the American Association for Cancer Research. 2005; 11:1815–20. [PubMed: 15756004]

43. Zheng Y, Basel D, Chow SO, Fong-Yee C, Kim S, Buttgereit F, et al. Targeting IL-6 and RANKL signaling inhibits prostate cancer growth in bone. Clinical & experimental metastasis. 2014; 31:921–33. [PubMed: 25223386]
44. Wu B, Crampton SP, Hughes CC. Wnt signaling induces matrix metalloproteinase expression and regulates T cell transmigration. Immunity. 2007; 26:227–39. [PubMed: 17306568]
45. Nemeth JA, Yousif R, Herzog M, Che M, Upadhyay J, Shekarriz B, et al. Matrix metalloproteinase activity, bone matrix turnover, and tumor cell proliferation in prostate cancer bone metastasis. Journal of the National Cancer Institute. 2002; 94:17–25. [PubMed: 11773278]
46. Gohji K, Fujimoto N, Hara I, Fujii A, Gotoh A, Okada H, et al. Serum matrix metalloproteinase-2 and its density in men with prostate cancer as a new predictor of disease extension. International journal of cancer Journal international du cancer. 1998; 79:96–101. [PubMed: 9495366]
47. Moses MA, Wiederschain D, Loughlin KR, Zurakowski D, Lamb CC, Freeman MR. Increased incidence of matrix metalloproteinases in urine of cancer patients. Cancer research. 1998; 58:1395–9. [PubMed: 9537238]
48. Kossakowska AE, Edwards DR, Prusinkiewicz C, Zhang MC, Guo D, Urbanski SJ, et al. Interleukin-6 regulation of matrix metalloproteinase (MMP-2 and MMP-9) and tissue inhibitor of metalloproteinase (TIMP-1) expression in malignant non-Hodgkin's lymphomas. Blood. 1999; 94:2080–9. [PubMed: 10477738]
49. Evans AL, Faial T, Gilchrist MJ, Down T, Vallier L, Pedersen RA, et al. Genomic targets of Brachyury (T) in differentiating mouse embryonic stem cells. PloS one. 2012; 7:e33346. [PubMed: 22479388]
50. Abrahams A, Parker MI, Prince S. The T-box transcription factor Tbx2: its role in development and possible implication in cancer. IUBMB life. 2010; 62:92–102. [PubMed: 19960541]

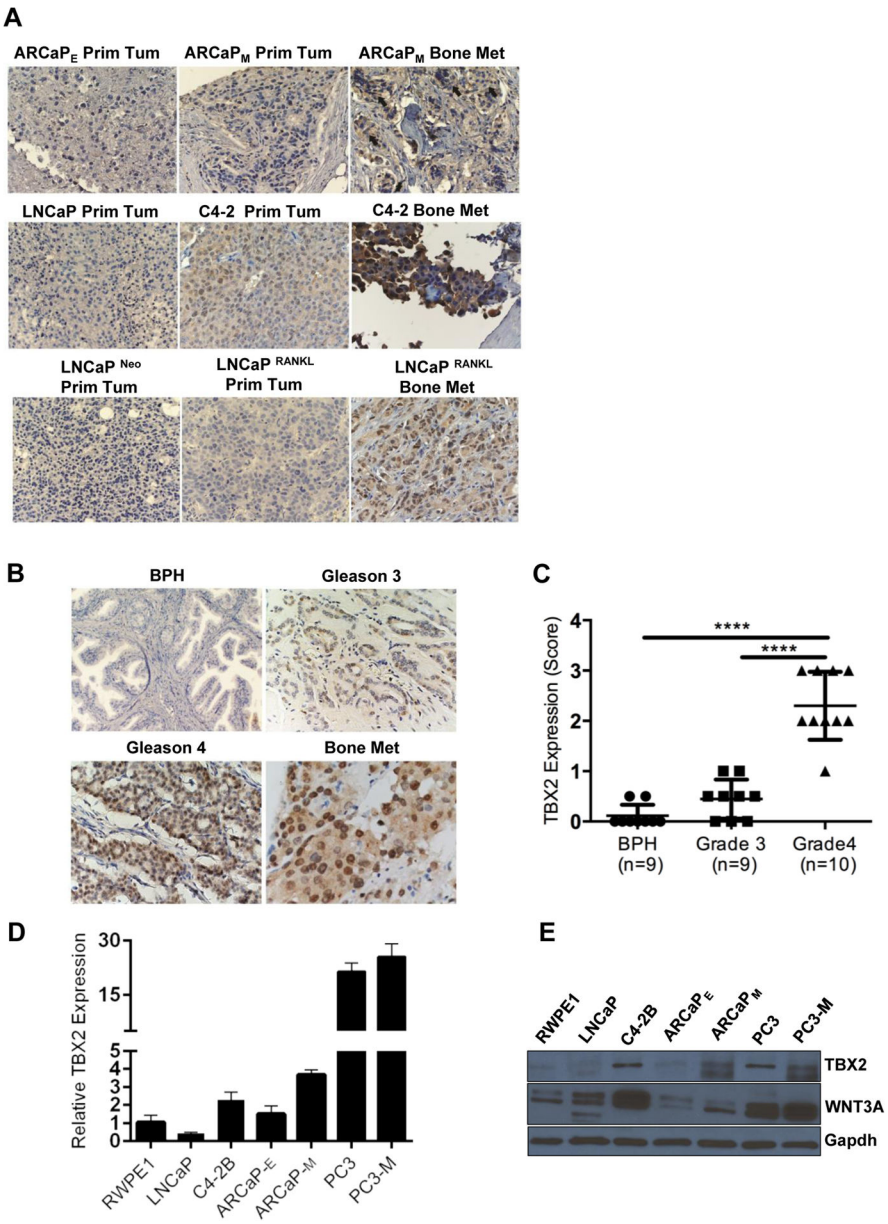

Figure 1. TBX2 is overexpressed in human PCa cell lines, tumor xenografts and clinical specimens, and its expression correlates with the potential to metastasize to bone and soft tissues

(**A**) Immunohistochemical staining showing correlation of TBX2 with [ARCaP$_E$ – ARCaP$_M$], [LNCaP – C4-2], and [LNCaP ^{Neo} – LNCaP ^{RANKL}] bone metastasis models. (**B**), (**C**) Increased TBX2 expression in high gleason grade PCa compared with low gleason grade PCa and BPH. Original magnification, × 250. $^{****}P<0.0001$. Further analysis showed that TBX2 in BPH and Gleason score 6 (3+3) is lower than in Gleason 7 (3+4 or 4+3) and Gleason 8 (4+4), $p<0.05$. Bone metastasis was positive in 5 of 7 specimens, Original magnification, × 500. (**D**) Extracts from PCa cell lines RWPE1, LNCaP, C4-2B ARCaP$_E$, ARCaP$_M$, PC3 and PC3-M were analyzed for the expression of TBX2 by qPCR (mean ± SEM, n=3). (**E**) Extracts from PCa cell lines RWPE1, LNCaP, C4-2B ARCaP$_E$, ARCaP$_M$,

PC3 and PC3-M were analyzed for the expression of TBX2 and WNT3A by immunoblotting.

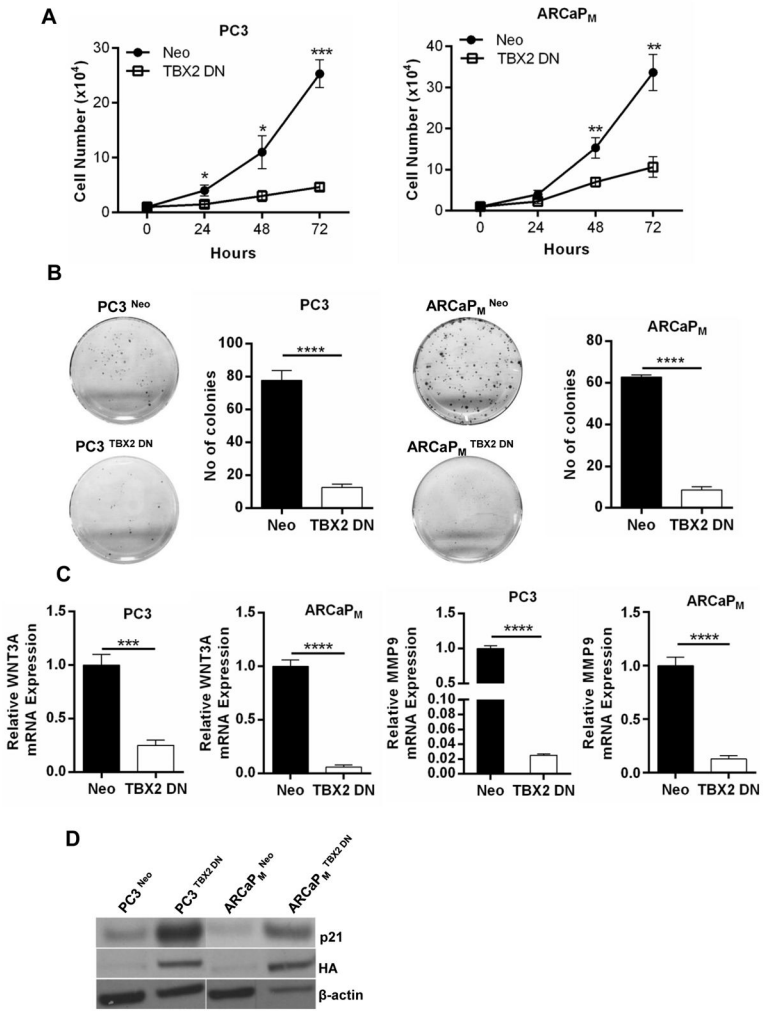

Figure 2. Identification of WNT3A and MMP9 as downstream effectors of the TBX2 signaling axis

(**A**) Growth curves of PC3 and ARCaP$_M$ cells (Neo and TBX2 DN) (mean ± SEM, n=3). (**B**) Colony formation of PC3 and ARCaP$_M$ cells (Neo and TBX2 DN) (mean ± SEM, n=3). (**C**) q PCR analysis of WNT3A and MMP9 in PC3 and ARCaP$_M$ cells (Neo and TBX2 DN) (mean ± SEM, n=3). (**D**) Immunoblots of PC3 and ARCaP$_M$ cells (Neo and TBX2 DN) for p21 and HA.

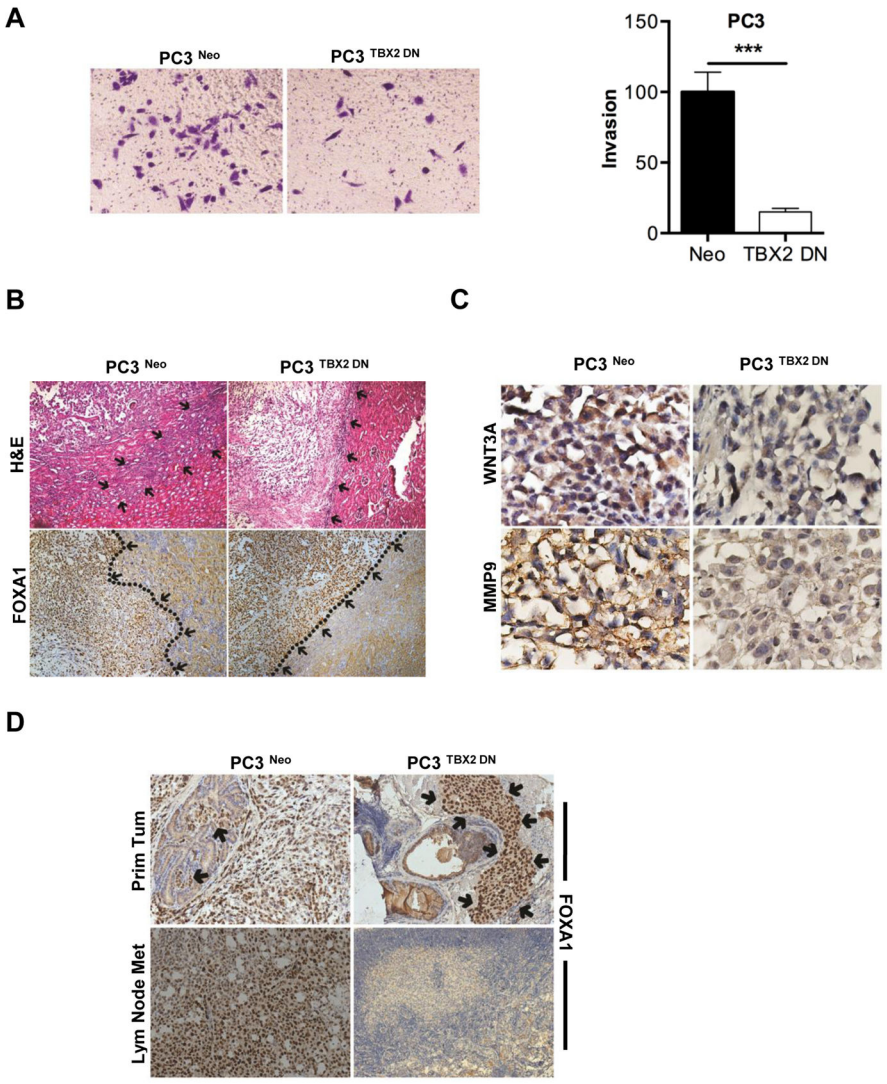

Figure 3. Blocking endogenous TBX2 in prostate cancer cells reduces local tumor invasion and metastasis

(**A**) PC3 cells (Neo and TBX2 DN) were assessed for their ability to invade. Data normalized to control and represents the mean ± SEM (n=3). (**B**) H&E and IHC analysis of FOXA1 in sub-renal capsule xenografts of PC3 cells (Neo and TBX2 DN). Arrows indicate tumor-kidney interface. Representative images from 6 different samples are shown. Original magnification, × 250. (**C**) IHC analysis of WNT3A and MMP9 in sub-renal capsule xenografts of PC3 cells (Neo and TBX2 DN). Representative images from 6 different samples are shown. Original magnification, × 250. (**D**) Upper panels show IHC analysis of FOXA1 in primary orthotopic xenograft tumors of PC3 cells (Neo and TBX2 DN). Arrows indicate tumor xenograft. Lower panels show IHC analysis of FOXA1 in lymph nodes obtained from mice orthotopically xenografted with PC3 cells (Neo and TBX2 DN). Representative images from 6 different samples are shown. Original magnification, × 250.

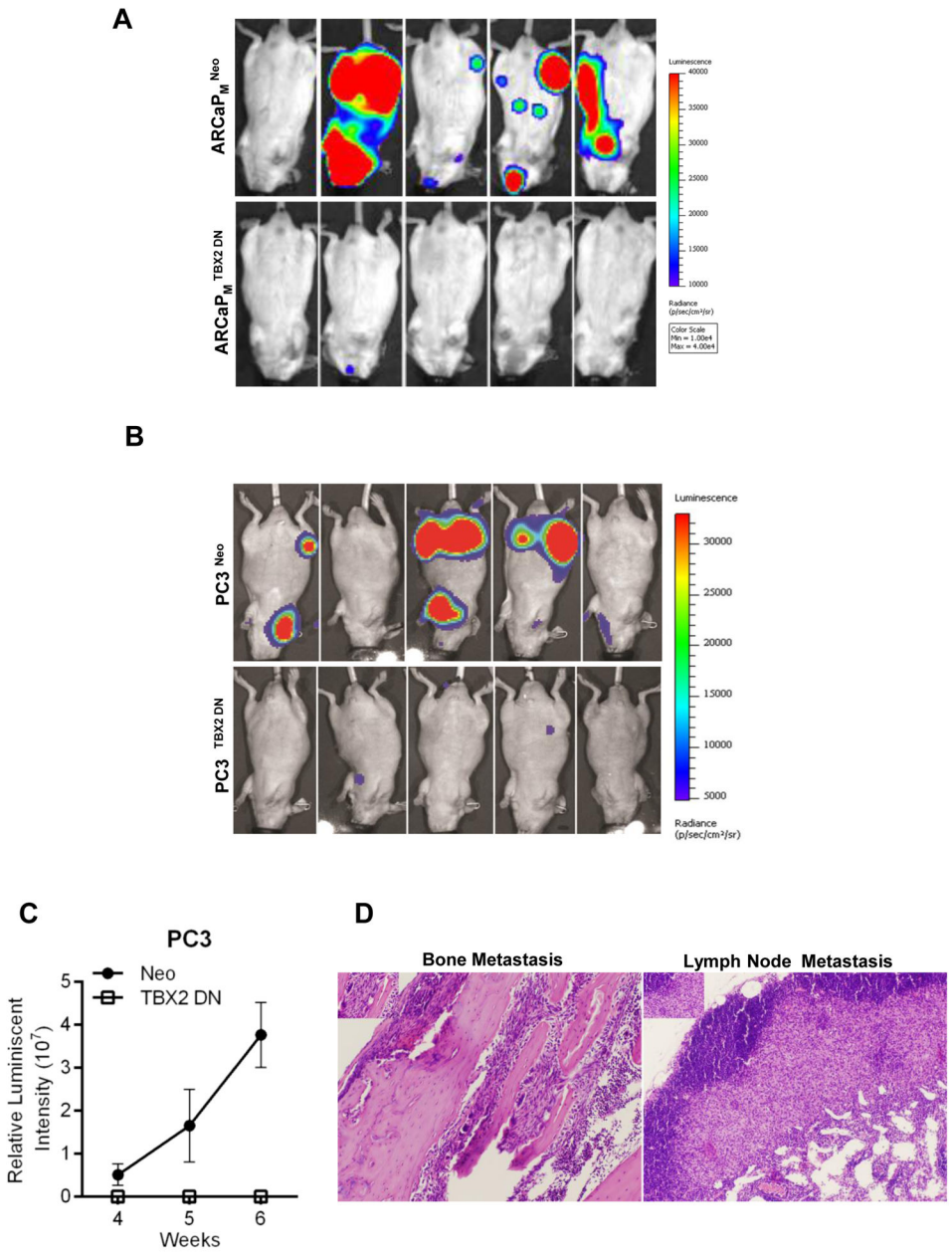

Figure 4. Dominant negative TBX2 expression in PCa cells abrogates cancer bone metastasis

(**A**) Representative BLI (week 8) images of 5 of 10 mice in each group from mice intra-cardially injected with ARCaP$_M$ cells (Neo and TBX2 DN). (**B**) Representative BLI (week 5) images of 5 of 10 mice in each group from mice intra-cardially injected with PC3 cells (Neo and TBX2 DN). (**C**) Normalized BLI curves of metastasis development for each experimental group from **B.** Data represent the mean ± SEM (n=10). (**D**) H&E analysis of bone and lymph node metastases from **B** (mice injected with PC3-Neo cells).

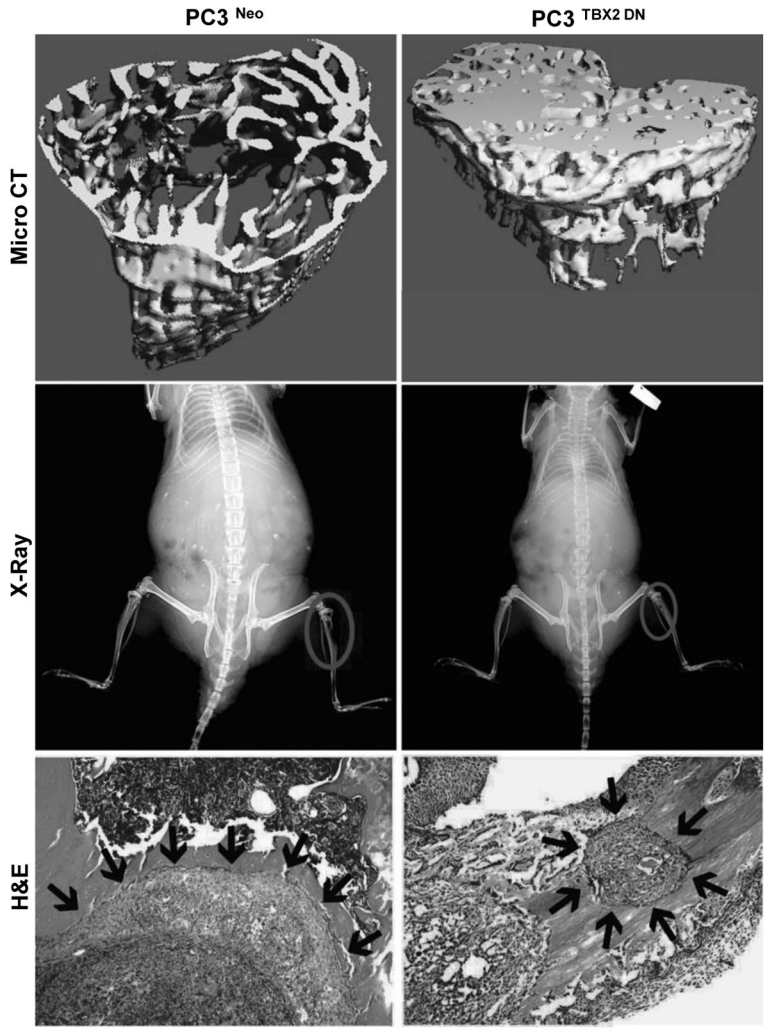

Figure 5. Dominant negative TBX2 alters PCa bone remodeling

A, Micro CT, X-Ray and H&E images of mice intra-tibially inculated with PC3 cells (Neo and TBX2 DN). Representative images from 6 different samples are shown.

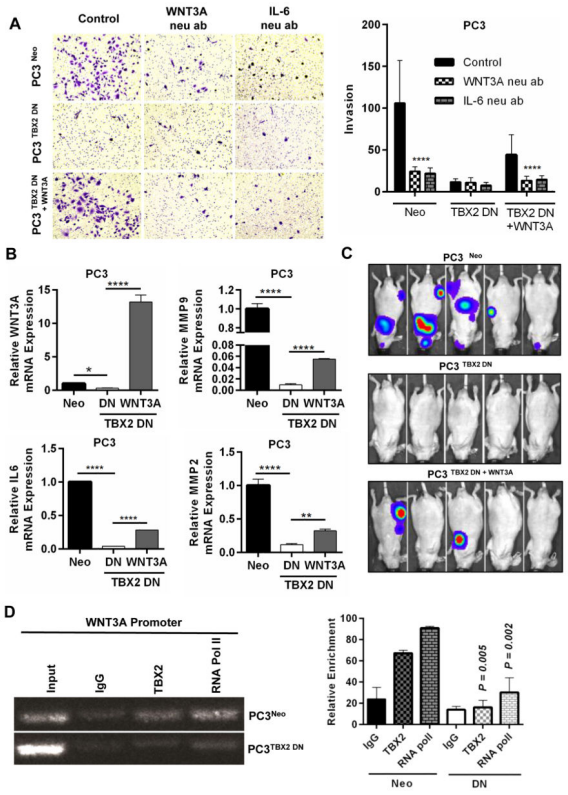

Figure 6. WNT3A, a downstream target gene of TBX2, mediates PCa bone metastasis

(**A**) PC3 cells (Neo, TBX2 DN and TBX2 DN + WNT3A) were assessed for their ability to invade with control (IgG ab), or addition of WNT3A neutralizing antibody (10 μg/ml), or IL-6 neutralizing antibody (150 ng/ml). Data represent the mean ± SEM (n=3). (**B**) q real-time RT-PCR analysis of WNT3A, MMP9, MMP2 and IL6 in PC3 cells (Neo, TBX2 DN and TBX2 DN + WNT3A) (mean ± SEM, n=3). (**C**) Representative BLI (week 5) images of 5 of 10 mice in each group from mice intra-cardially injected with PC3 cells (Neo, TBX2 DN and TBX2 DN + WNT3A). (**D**) Chromatin immunoprecipitation analysis (ChIP) of PC3 cells (Neo, TBX2 DN) showing *in vivo* binding of TBX2 on WNT3A promoter (mean ± SEM, n=3).

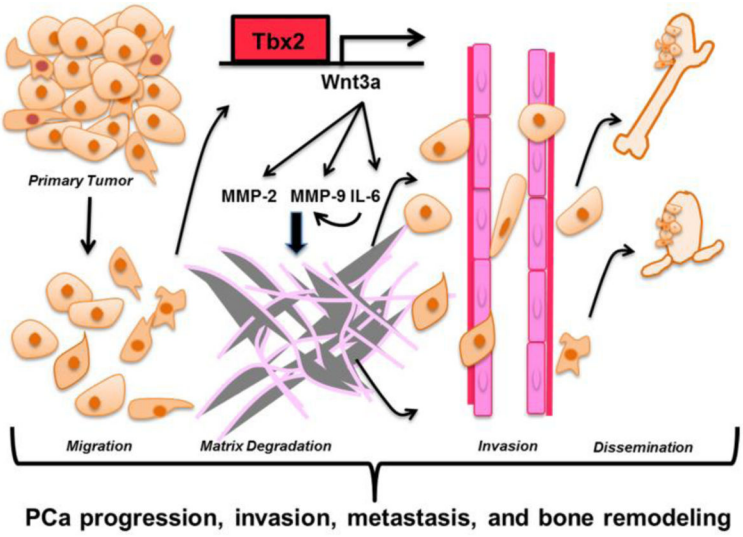

Figure 7. Proposed model depicting the mechanism of action of TBX2 in the PCa progression cascade

A proposed working model on how TBX2 affects PCa progression, invasion, metastasis, and bone remodeling by engaging WNT3A. TBX2 transcriptionally regulates WNT3A that in turn induces MMP9, MMP2 and IL-6 - factors known to play critical roles in tumor invasion and metastasis.